Aerial Infrared Thermography of a Utility-Scale PV Plant After a Meteorological Tsunami in Brazil

Aline Kirsten Vidal de Oliveira[1], Mohammadreza Aghaei[2], Uzoma Edward Madukanya[2], Lucas Nascimento[1], Ricardo Rüther[1]

[1]Universidade Federal de Santa Catarina, Florianópolis-SC, 88040-900, Brazil
[2]University of Freiburg, Freiburg im Breisgau, 79085, Germany

***Abstract* — Aerial Infrared Thermography (aIRT) is a non-destructive and cost-effective method for detecting faults in large-scale PV plants. In this paper, a 1 MW multi-crystalline PV plant-block that was hit by a meteorological tsunami in Brazil in 2016, is inspected systematically using the aIRT method. The main objective was to validate this inspection technique for commercial application. Various failures like hotspots, bypassed substrings, short-circuited and disconnected PV strings were detected at the PV plant using aIRT inspection in less than one hour. The results have proven that this semi-autonomous method is very fast, reliable and effective for large scale PV plants.**

***Index Terms* — Unmanned Aerial Vehicle (UAV), Aerial Infrared thermography (aIRT), Photovoltaic (PV) Plant, Fault Inspection.**

I. Introduction

Photovoltaic (PV) is currently the fastest growing energy generation technology worldwide, and has begun to spread as well in the so-called sunbelt countries. Brazil is one of the largest countries in that region and bears an immense solar potential, combined with relatively high electricity tariffs. The benchmark of 1 GW of installed PV capacity was achieved in the end of 2017, and utility-scale PV power plants are beginning to gain attraction in the government-led energy auctions system [1], [2].

The dominating paradigm for PV systems seems to be shifting from decentralized PV installations to utility-scale PV plants. In Latin America, PV plants account for 90% of the total installed PV capacity [1]. The system size of these PV plants are often in the double-digit megawatt range or even beyond.

Performance and reliability of PV plants become more relevant for grid stability and financial revenue for the investors. Therefore, operation and maintenance (O&M) schemes have been established for ensuring safety, availability and productivity of the PV plants [3]–[5]. Early fault detection can contribute to maintain high power availability and avoid outages or costly maintenance measures. In the past 10 years, sophisticated inspection methods and techniques have been developed for performance assessment [6]. Among them, real-time monitoring, I-V curve tracing and infrared thermography (IRT) are the most precise and practical methods. In particular, IRT is one of the primary choices for fault inspections, and has proven to be reliable and cost-effective [7]. It requires only a minimum of instrumentation and is carried out under operation conditions, i.e. without interrupting the energy generation of the PV plant. Furthermore, it is possible to detect nearly all types of defects in PV cells and modules, since these defects have an influence on the recombination of charge carriers and in consequence, on the thermal behavior of PV modules [7]. Additionally, IRT can provide information about the exact physical location of a defect.

Traditionally, IRT is conducted on-site with a portable infrared (IR) camera, or on a lifting system in order to increase the vision range. The large geographical size of utility-scale PV plants, however, presents a great challenge for applying IRT. In the traditional way, IRT application becomes time-consuming and labor-intensive. Therefore, it is usually limited to randomly selected areas of a PV plant. In order to apply the IRT inspection to the entire PV plant, the combination with aerial inspection techniques by unmanned aerial vehicles (UAV) has been proposed [2], [8]–[12]. Regarding the development stage of this method, aerial infrared thermography is still in the early commercialization phase. The reputation as a reliable and effective inspection method needs to be consolidated, in order to promote further scaling. This paper provides a systematic approach for the validation of the potential and applicability of aerial IRT for fast fault detection on a 1 MW multi-crystalline PV plant-block, located in the South of Brazil, which was damaged during an extreme climatic event denominated meteorological tsunami.

II. Aerial Infrared Thermography

The application of UAV for monitoring services in the energy sector has become popular and is used for tasks such as power line transmission and wind turbine inspection or gas and oil pipeline monitoring. Small or medium size UAV with a weight up to 25 kg are perfectly suited to carry infrared imaging sensors. Moreover, rotor-based UAV offers the possibility to fly at low altitudes, hover in place and to obtain precise imagery and the exact fault localization.

Aerial IRT operates on the same principle as traditional IRT except for the way of application. The recombination of charge carriers in PV cells causes a certain temperature distribution, which is homogenous throughout the whole PV module's surface under normal conditions. A defect changes this thermal distribution and therefore enables the detection of malfunctioning PV cells or modules, using an infrared camera. The IRT camera captures radiation emitted in the infrared

wavelength spectrum between 1.4 µm and 15µm. The infrared thermography employed for PV applications usually detects wavelengths in the long-infrared wavelength range of 7 – 14 µm, which is an equilibrium between costs, availability and measuring conditions of IRT sensors [13].

Aerial IRT (aIRT) is therefore a very attractive method for reliable, fast and cost-efficient inspection of large-scale PV plants. Moreover, it can add to elaborate precise 'fault maps' that simplifies the selection and organization of maintenance measures. Additionally, visual images can be captured simultaneously, in order to complete the IRT inspection by covering that kind of faults that cannot be detected with IRT, such as discoloration defects.

III. Site Description

The experimental site is a 3 MW PV R&D power plant called "Cidade Azul", which is located in the city of Tubarão, in the state of Santa Catarina, in South of Brazil (28° South, 49° West), and was constructed for research and development purposes in 2014. Fig. 1 shows a picture of the fully-monitored PV plant, which consists of three different PV technologies, divided in blocks of 1 MW each – namely multi-crystalline (mc-Si) PV modules at the back of the picture next to the wind turbine, followed by thin-film CIGS (Copper Indium Gallium Diselenide) modules in the middle, and thin-film amorphous-microcrystalline silicon (a-Si) modules at the North (front) end. The PV modules are fixed on ground-mounted racks tilted at 30 degrees, facing true North.

Fig. 1. 3 MW R&D utility-scale PV Plant in Brazil.

In the end of 2016, a meteorological tsunami hit the coast of the region, where the plant is located. During this phenomenon, wind gusts, measured by the wind tower next to the plant, reached up to 210 km/h. This extreme climatic event has created great havoc and caused damages to the PV power plant. However, the damages remained moderate and only 0.1% of the 20 thousand PV modules were detached from their ground-mounted metal structures; also, several PV arrays had their electrical wiring compromised by the storm. In order to achieve a quick analysis on the overall condition of the PV plant, a fault inspection campaign was carried out using aerial IRT. The experiment was focused on the 1 MW multi-crystalline PV plant-block that is composed of 4,199 Yingli Solar 245Wp multi-crystalline PV modules.

IV. Experimental Setup

The aerial inspection was carried out with a model DJI Phantom 3 Professional UAV, which has been modified and equipped with a lightweight (80g) infrared camera. Therefore, the standard UAV camera was substituted with the high resolution, 640x480 pixel, infrared camera from Thermoteknix, which uses an amorphous silicon IRT detector to operate in the long-infrared wavelength spectrum between 7 and 14 µm. For image transmission, the original telemetry system had to be removed and substituted as well, because its communication protocol was incompatible with the analog video signal produced by the IRT camera. In lieu, a Boscam first-person-view (FPV) video transmitter, with a transmission power of 1W, was implemented to transmit the IRT images to a USB receptor, allowing the visualization and recording of the images on a computer. In order to achieve a good transmission quality from any spatial position, a 5.8 GHz Cloverleaf antenna with a spherical radiation pattern was applied. Fig. 2 shows the developed aerial IRT-measurement UAV.

Fig. 2. The aerial IRT-measurement UAV developed.

For the aIRT assessment, the UAV was remotely piloted in a certain altitude above the PV modules to detect the failures and defects. The captured IRT images were transmitted to the computer via the radio frequency antenna. Subsequently, the IRT images were compared to standardized thermal patterns that have been validated by the International Electrotechnical Commission (IEC), in order to achieve ad-hoc analyses on the health state of the PV plant. Fig. 3 illustrates the procedures used for the aIRT inspection.

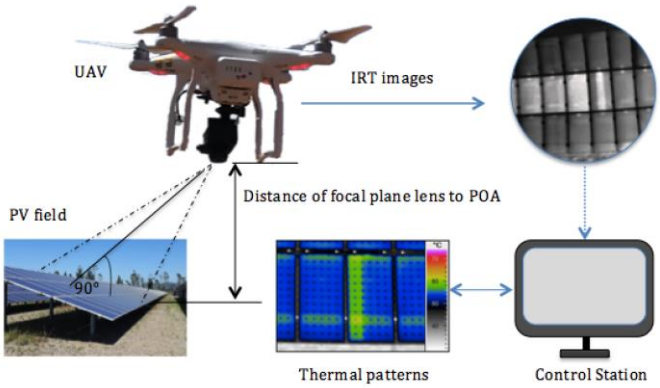

Fig. 3. Scheme of the aIRT measurement procedure

The flight settings, such as altitude, speed and angle of view (AOV) of the IRT camera were set according to experiences of previous studies [10], [14], [15]. In order to avoid smearing effects on the IRT images, which occur when the flight speed is higher than the imaging speed and might lead to misinterpretations, a flight velocity of maximum 3 m/s was adopted. AOV on the PV array should be perpendicular since the emissivity and reflectivity of the PV module's surface are respectively at the highest and lowest point at 90° [16], [17].

In a second stage of the experiment, a detailed investigation on the detected faults was carried out in order to quantify the effect on the performance of the PV module or string.

Therefore, a performance analysis with I-V curve measurements has been performed for the affected PV modules and the affected strings, with an uncertainty smaller than 1%. Additionally, IRT images were taken with a portable FLIR T640 IRT camera, in order to analyze the temperature differences and absolute temperatures.

V. Experimental Results

The aerial inspection was carried out under stable thermal state conditions with a mean irradiance above 800W/m2 at the plane of array (POA), clear sky and a cloud coverage of maximum 2/8 cumulus, and mean wind speeds below 3m/s. Thus, the minimum requirements for outdoor infrared thermography for PV systems defined by IEC 64266-3:2017 [18] were respected.

The initial flight altitude of 6m allowed the detection of defects on the PV module level. The flight altitude corresponds to the distance of the focal plane lens of the IRT camera to the POA. Above 20m, the field of view (FOV) was increased, but, at the same time, the detectability of PV module level faults was decreased. Fig. 4, 5 and 6 illustrate IRT images of the same damaged PV module with two hotspots and a bypassed substring at different altitudes. At 6m and 10m, the defects are clearly visible. The bypassed substring and the hotspot with the lower temperature are hardly perceptible at the altitude of 20m. However, only the hotspot with the higher temperature is still easily detected.

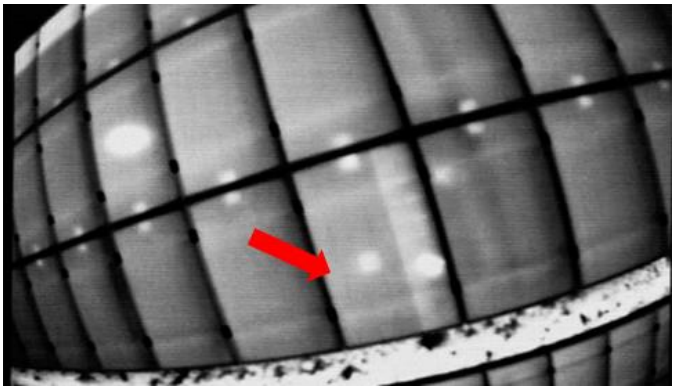

Fig. 4. IRT image of damaged PV module with two hotspots and a bypassed substring, clearly visible at an altitude of 6m.

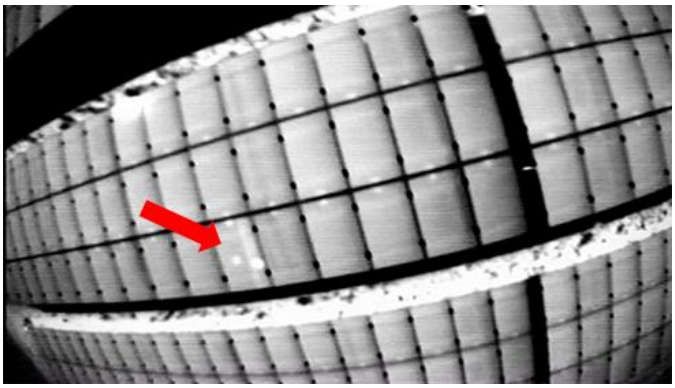

Fig. 5. IRT image of damaged PV module, with two hotspots and a bypassed substring, visible at an altitude of 10m.

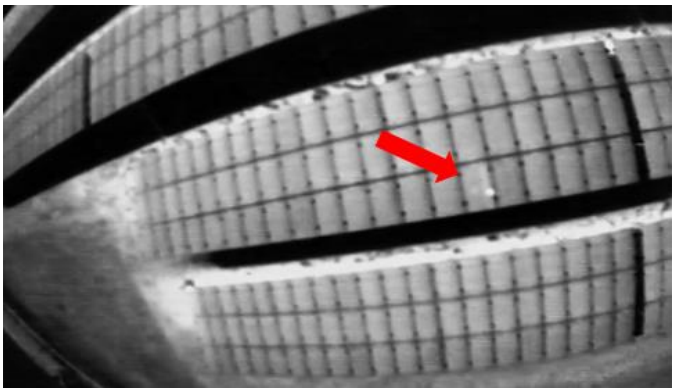

Fig. 6. IRT image of damaged PV module, with one clearly visible hotspot and one hotspot and a bypassed substring that are hardly perceptible at an altitude of 20m.

The detailed investigation with the handheld IRT camera revealed a considerable high-temperature difference of 39.3°C between the two hotspots. The absolute temperature of the hotspots was respectively 62.1°C and 101.4°C, compared to

58.4°C of a healthy cell, shown in Fig. 7. This might explain why the high-temperature hotspot is still well visible at 20m and gives hint to a correlation between altitude and hotspot fault detectability, in dependence on the temperature level. The temperature difference of the low-temperature hotspot to a healthy cell is only 3.7°C.

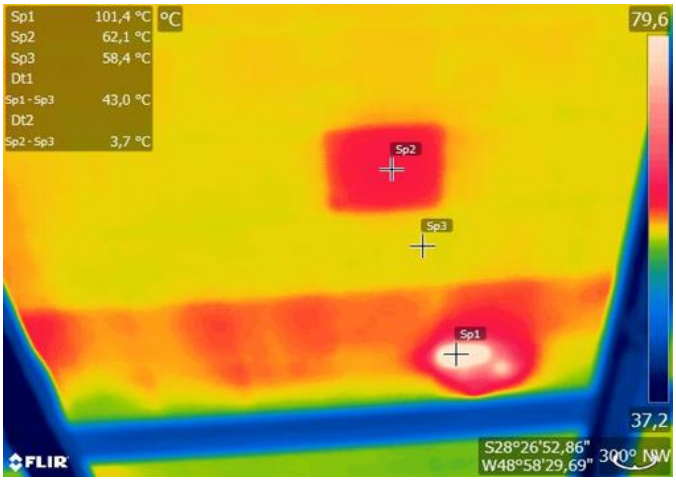

Fig. 7. Radiometric IRT image of damaged PV module with two hotspots and a bypassed substring, presenting temperature differences of 43°C and 3.7°C, respectively.

After gathering data of all detected hotspots and bypassed substrings, the histogram presented in Fig. 8 was plotted. It shows that most of the damaged modules detected presented a temperature difference greater than 30ºC on their surface. This indicates that most of the defects could be detected much faster if taken from a higher altitude.

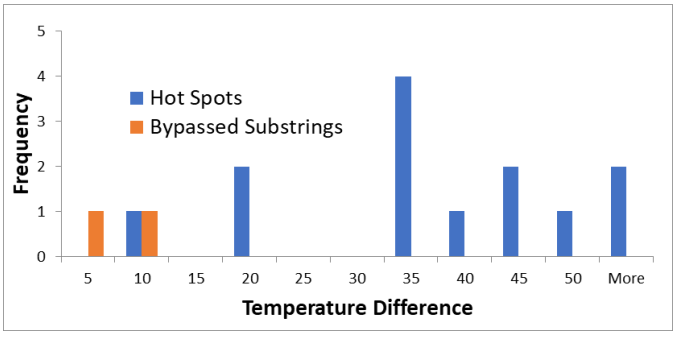

Fig. 8. Histogram of temperature differences between defective and healthy cell.

PV array level faults like disconnected modules or short-circuited strings remain clearly visible even at high altitudes and a relatively low temperature difference. Fig. 9 depicts an IRT image at an altitude of 100m. The temperature of the disconnected PV strings differs only slightly (1.9°C) from the temperature of the functioning strings.

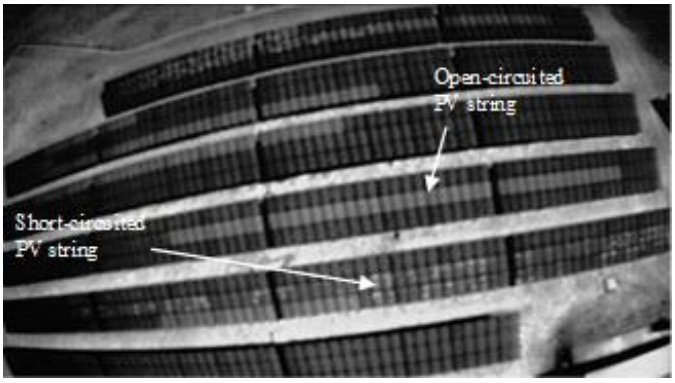

Fig. 9. IRT image at an altitude of 100m. Open-circuited and short-circuited PV strings are easily visible.

The pie diagram in Fig. 10 presents the results of the aIRT inspection with the proposed scheme. Altogether 54 defects were detected during the PV plant inspection. Disconnected PV strings, short-circuited PV strings and PV module level defects account for approximately 1/3 of the detected defects in equal parts. Defects on the PV module level can be subdivided into hotspots that make up the major part (26%) and bypassed substrings (4%). The inspection time for the 1MW multi-crystalline PV plant-block was 1 hour.

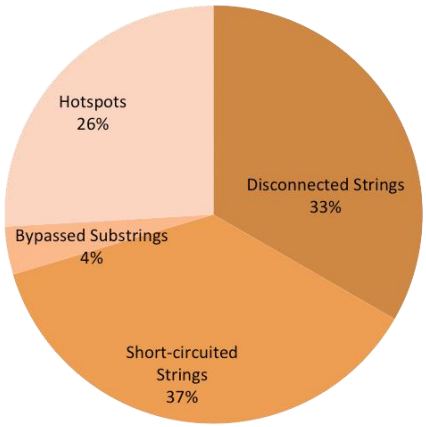

Fig. 10. Summary of detected failures.

The ad-hoc analysis was carried out simultaneously to the flight by a second inspector. On basis of the thermal patterns, the identified faults were classified and registered in a fault map that charted the exact location in the PV plant's string plan.

Fig. 11 presents different IRT images classified with the corresponding thermal patterns described in the IEC 62446-3 [18]. In Fig. 11-(a), an IRT image of a disconnected PV string is shown. The temperature of the disconnected PV string is higher in comparison to the functioning PV strings below and above, and homogeneously distributed over the PV modules' surfaces. In a grey-scale pallet, IRT images with higher temperatures are indicated by a brighter grey shade. Therefore, the affected modules appear brighter in the IRT image.

During the investigation, several short-circuited strings have been detected, as seen in Fig. 11-(b). This fault is characterized by a randomly distributed temperature pattern. Fig. 11-(c) depicts an aerial IRT image of a PV module with a bypassed substring in comparison to the corresponding standardized thermal pattern. On the same image, left to that faulty module, open-circuited modules are also visible.

Other types of faults on PV cell or module level, such as micro-cracks, faulty cell interconnections, shading or broken glass appear as hotspots in the IRT image, since in defective areas the PV module becomes reversed biased and heats up. An example is shown in Fig. 11-(d).

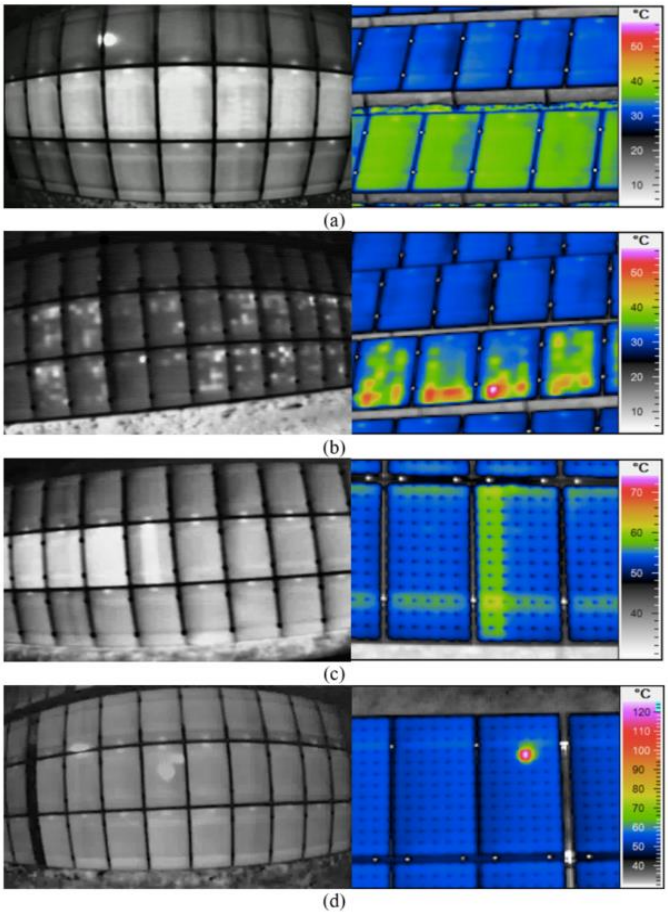

Fig. 11. IRT images of damaged modules compared to the corresponding IEC thermal patterns (a) disconnected string (b) short-circuited strings (c) bypassed substring of PV module (d) overheated PV cell.

The identification and classification of defects according to their thermal pattern is quite straightforward. However, influences on the thermal images, e.g. experimental artifacts such as self-shading or reflection interferences, have to be considered. In Fig. 12 an IRT image with experimental artifacts is presented to exemplify the issue. The depicted reflection might be mistaken for a hotspot.

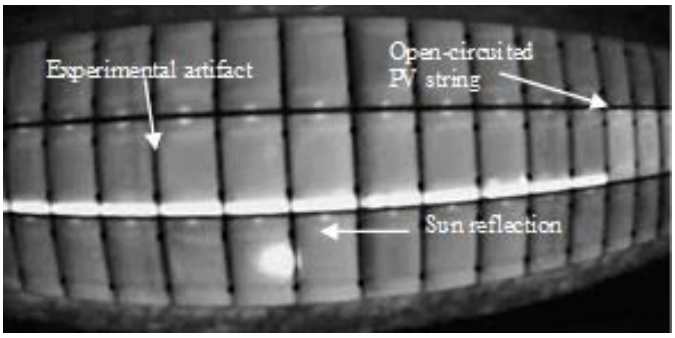

Fig. 12. IRT image of PV modules presenting experimental artifacts.

The electrical impact of a defect on the performance of a PV module depends on shape, size, location, and duration of the fault. In order to quantify the effect of the detected defects electrically, I-V curve measurements were carried out. The I-V curve in Fig. 13 presents an inflection point at approximately 20V. The resulting stepped form of the I-V curve is an indication of an active bypass diode over 1/3 of the series connected solar cells. Additionally, a steep slope near the open-circuit voltage can be noticed, indicating a strong increase of the series resistance. In fact, the affected PV cell presents strong burn marks at the backsheet, caused by broken interconnect busbars. The power loss is significantly high at over 45%. The visual representation of the I-V curve corresponds well with the thermal image from the aIRT inspection that revealed a bypassed substring and two hotspots (Fig. 4).

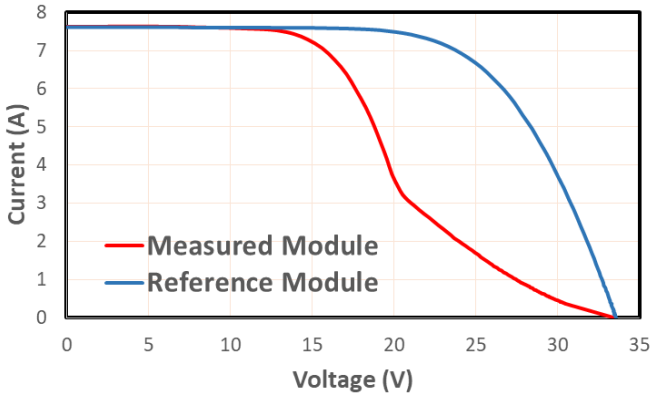

Fig. 13. I-V curve of a PV module with a bypassed substring.

The I-V curve assessment helped to quantify the electrical impact of the detected faults. The electrical effect of a bypassed substring is strong, causing severe performance losses, in the range of 40%. On the contrary, the impact caused by hotspots turned out to be diverse and less expressive. The performance losses caused by the analyzed defects reached up to 25%.

However, the electrical impact of a defect on a single PV module becomes relativized when considering the whole PV string. For the analyzed cases, the performance losses of the

affected PV string, which consists of 20 series connected modules, are only marginal and range between 1.5 and 3%. This has to be considered when drawing conclusions based on the aerial IRT inspection technique.

V. Conclusion

In this paper a semi-autonomous method for the fault inspection of the damaged PV power plant has been proposed. It proved to be practical and effective. Since there is no need for intervening in the PV plant operation, the inspection can be carried out much faster in comparison with traditional inspection methods, and at a reasonably low cost.

A number of 54 defects and failures have been detected, using the proposed method, in less than one hour. The majority of the defects were detected on the PV array level, namely short-circuited and disconnected PV strings. However, a quarter of the detected defects were hotspots caused by partial shading, broken glass, delamination and broken interconnections.

The accuracy of the method depends strongly on the resolution of the IRT sensor and the flight altitude. The research has shown that the detectability of defects with a low temperature level, compared to healthy parts of the PV module, is more reliable at low altitudes between 6m and 10m. Consequently, depending on the required granularity/precision, the altitude can be varied in order to accelerate the inspection and to focus on pre-defined defects.

The ad-hoc analysis, i.e. classifying the defects by means of standardized thermal patterns, enabled the exact localization of defects in the string plan and the elaboration of a 'fault map'. This map can serve to locate defects instantaneously and to conduct further investigations, or to take immediate measures if considered necessary. Additionally, estimations about the electrical impact based on the thermal pattern can be made. However, conclusions on the overall performance losses due to the detected defects have to be drawn carefully.

Acknowledgement

RR wishes to acknowledge with thanks the Alexander von Humboldt Foundation for a Research Linkage project grant that allowed the acquisition of the IR camera used in this work.

References

[1] M. Parikh, "Latin America PV Playbook," GTM Research, pp. 7–10, 2016.

[2] C. Cioaca, S. Pop, E. C. Boscoianu, and M. Boscoianu, "Aerial Infrared Thermography: A scalable procedure for photovoltaics inspections based on efficiency and flexibility," *Applied Mechanics and Materials*, vol. 772, no. July 2015, pp. 546–551, 2015.

[3] V. Papaeconomou; S. Degener, "Operation & Maintenance – Best practices guidelines / Version 2.0," Solar Power Europe, pp. 34–38, 2017.

[4] T. Keating, A. Walker, and K. Ardani, "Best practices in PV system operations and maintenance," National Renewable Energy Laboratory, pp. 30–60, 2015.

[5] A. Woyte, M. Richter, D. Moser, S. Mau, N. Reich, and U. Jahn, "Monitoring of photovoltaic systems: Good practices and systematic analysis," *Journal of Chemical Information and Modeling*, vol. 53, no. 9, pp. 1689–1699, 2013.

[6] A. Triki-Lahiani, A. Bennani-Ben Abdelghani, and I. Slama-Belkhodja, "Fault detection and monitoring systems for photovoltaic installations: A review," *Renewable and Sustainable Energy Reviews*, vol. 82, no. July 2017, pp. 2680–2692, 2018.

[7] C. Buerhop, D. Schlegel, M. Niess, C. Vodermayer, R. Weißmann, and C. J. Brabec, "Reliability of IR-imaging of PV-plants under operating conditions," *Solar Energy Materials and Solar Cells*, vol. 107, pp. 154–164, 2012.

[8] F. Grimaccia, S. Leva, A. Dolara, and M. Aghaei, "Survey on PV modules' common faults after an O&M flight extensive campaign over different plants in Italy," *IEEE Journal of Photovoltaics*, vol. 7, no. 3, pp. 810–816, 2017.

[9] C. Buerhop, T. Pickel, M. Dalsass, H. Scheuerpflug, C. Camus, and C. J. Brabec, "AIR-PV-check: A quality inspection of PV-power plants without operation interruption," *Conference Record of the IEEE Photovoltaic Specialists Conference*, vol. 2016–Novem, pp. 1677–1681, 2016.

[10] M. Aghaei, "Novel methods in control and monitoring of photovoltaic systems," Ph.D thesis, Politecnico di Milano, 2016.

[11] F. Grimaccia, M. Aghaei, M. Mussetta, S. Leva, and P. B. Quater, "Planning for PV plant performance monitoring by means of unmanned aerial systems (UAS)," *International Journal of Energy and Environmental Engineering*, vol. 6, no. 1, pp. 47–54, 2015.

[12] M. Dalsass, H. Scheuerpflug, F. W. Fecher, C. Buerhop-Lutz, C. Camus, and C. J. Brabec, "Correlation between the generated string powers of a photovoltaic: Power plant and module defects detected by aerial thermography," *Conference Record of the IEEE Photovoltaic Specialists Conference*, vol. 2016–Novem, pp. 3113–3118, 2016.

[13] I. Tsanakas and P. N. Botsaris, "On the detection of hot spots in operating photovoltaic arrays through thermal image analysis," *Materials Evaluation*, vol. 71, no. April, pp. 457–465, 2013.

[14] M. Aghaei, F. Grimaccia, C. A. Gonano and S. Leva, "Innovative automated control system for PV fields inspection and remote control," *IEEE Transactions on Industrial Electronics*, vol. 62, no. 11, pp. 7287–7296, 2015.

[15] P. B. Quater, F. Grimaccia, S. Leva, M. Mussetta, and M. Aghaei, "Light Unmanned Aerial Vehicles (UAVs) for cooperative inspection of PV plants," *IEEE Journal of Photovoltaics*, vol. 4, no. 4, pp. 1107–1113, 2014.

[16] C. Buerhop, U. Jahn, U. Hoyer, B. Lercher, and S. Wittmann, "Abschlussbericht Machbarkeitsstudie Überprüfung der Qualität von Photovoltaik- Modulen mittels Infrarot-Aufnahmen," ZAE Bayern e.V., pp. 1–46, 2007.

[17] S. Leva, M. Aghaei, and F. Grimaccia, "PV power plant inspection by UAS : Correlation between altitude and detection of defects on PV modules," in *Environment and Electrical Engineering (EEEIC), 2015 IEEE 15th International Conference on*, 2015.

[18] International Electrotechnical Commission, "IEC TS 62446-3 - Photovoltaic (PV) systems - Requirements for testing, documentation and maintenance - Part 3: Photovoltaic modules and plants - Outdoor infrared thermography." Geneva, 2017.